CHAPTER 4

# ON TEMPERATURE-RATE DEPENDENT TWO-TEMPERATURE THERMOELASTICITY

## 4.1 Variational and Reciprocal Principles on the Temperature-Rate Dependent Two-Temperature Thermoelasticity Theory

### 4.1.1 Introduction[1]

This chapter is concerned with the study of the modified temperature-rate dependent two-temperature thermoelasticity theory. The concept of two-temperature theory was first introduced by Gurtin and Williams (1966). They have suggested that the entropy inequality requires a modification based on the distinction between two heat transfer mechanisms implying that the heat flux inside the body and the external heat supply are independent. Due to this distinction, the separation of entropy flow in the second law of thermodynamics was considered, by introducing two different temperatures: the thermodynamic temperature $\theta$ and the conductive temperature $\phi$, based on the same factor of proportionality. Further, Chen and Gurtin (1968) and then Chen et al. (1969)

[1]The content of this sub chapter is published in ***Journal of Thermal Stresses***, 43(7), 816-828 (2020)

derived the governing equations of the two-temperature theory of thermoelasticity by following this modified entropy inequality. They also demonstrated that the distinction between these two temperatures in a time independent situation is proportional to the heat supply and these two temperatures are identical when an external heat source is absent. They proposed a relation between these two temperatures and termed it as a two-temperature relation. Later on, taking into account this two-temperature relation, Youssef (2006) developed the two-temperature generalized thermoelastic model in the frame of LS model. The governing equations for the temperature-rate dependent two-temperature (TRDTT) thermoelasticity theory were also stated by Youssef (2006). Recently, Shivay and Mukhopadhyay (2019) employed generalized thermodynamics laws and presented a modified TRDTT thermoelasticity theory. The generalized two-temperature relation obtained in view of this modified TRDTT thermoelasticity theory reduces to the two-temperature relation provided by Youssef (2006) in a specific situation. The present chapter of the thesis consists of two subchapters, the objective of which is to analyze the modified temperature-rate dependent two-temperature thermoelasticity theory proposed by Shivay and Mukhopadhyay (2019).

The dynamical state of a system of thermoelasticity can be obtained from the variational principle by representing it as the extremum of a functional or function (Ignaczak and Starzewski (2010)). By combining initial conditions into the field equations, variational theorem has been introduced by Ignaczak (1963) and Gurtin (1964). Iesan (1966; 1974) and subsequently, Nickell and Sackman (1968b) derived variational theorem of convolution type for linear coupled thermoelastic models. Later on, the Gurtin type variational principle under consideration of microstructure based solid was presented by Iesan (1967). Moreover, numerous ways for integration of elasticity equations concerning the Green's function can be achieved by using the reciprocal principle. The reciprocal principle has convenient practical use in dealing with engineering problems (Nowacki (1975b)). Mayzel (1951) established the reciprocity theorem in thermoelastic-

ity theory in view of the static problem which is known as the Betti-Maxwell reciprocal principle. The reciprocity theorem in the uncoupled thermoelasticity theory and coupled thermoelasticity theory was established by Predeleanu (1959) and Ionescu-Cazimir (1964), respectively. Without making use of the Laplace transform, the reciprocal principle was derived by Iesan (1967). Later, Nowacki (1975b) also discussed the reciprocity theorem under coupled thermoelasticity theory concerning the homogeneous and anisotropic material. Without involving initial data into the field equation and excluding the use of Laplace transform, the reciprocity theorems were derived by Scalia (1990). Chandrashekharaiah and Srikantaiah (1983), Wang et al. (1997), and Chandrashekharaiah (1998b) established the variational principle, reciprocal principle, and uniqueness theorem on various generalized thermoelasticity theories. Convolution type variational and reciprocal principles under two-temperature LS theory were derived by Kumar et al. (2010). Chirita and Ciarletta (2010), Kumari and Mukhopadhyay (2017b) and subsequently, Gupta and Mukhopadhyay (2018) derived the convolution type variational principles and reciprocity theorems on various thermoelastic systems. Recently, Sachan et al. (2023) established the reciprocal and variational theorems on the TRDTT thermoelasticity theory.

In the present subchapter, variational theorem and reciprocity theorem are established in the context of the modified temperature-rate dependent two-temperature (MTRDTT) thermoelasticity theory proposed by Shivay and Mukhopadhyay (2019). Therefore, the subchapter has been organized in the following manner. We begin with summarizing the fundamental equations of MTRDTT for the homogeneous and anisotropic material and define a mixed initial-boundary value problem under non-homogeneous initial conditions. Further, an alternative characterization of the mixed initial-boundary value problem is presented including the initial conditions into the field equations. Lastly, a variational theorem and reciprocity theorem of convolution type are derived based on this formulation.

### 4.1.2 Basic Equations and Problem Formulation

We consider an anisotropic and homogeneous thermoelastic material occupying a regular region $B$ in three dimensional Euclidean space. The closure and boundary of $B$ are denoted by $\overline{B}$ and $\partial B$, respectively. Let $n_i$ represents the unit outward components normal to $\partial B$ and subsets of $\partial B$ are $\partial B_i$, $(i = 1, 2, 3, 4)$ such that

$$\partial B_1 \cup \partial B_2 = \partial B_3 \cup \partial B_4 = \partial B,$$
$$\partial B_1 \cap \partial B_2 = \partial B_3 \cap \partial B_4 = \phi.$$

Therefore following Shivay and Mukhopadhyay (2019), the governing equations and the constitutive relations under the MTRDTT thermoelasticity theory are given as follows:

**Equations of motion:**

$$\sigma_{ij,j} + F_i = \rho \ddot{u}_i. \tag{4.1.1}$$

**Energy balance equation:**

$$\rho H - q_{i,i} = \rho C_E \left(\dot{\theta} + \tau_2 \ddot{\theta}\right) + T_0 \gamma_{ij} \dot{e}_{ij}. \tag{4.1.2}$$

**Constitutive equations:**

$$\sigma_{ij} = C_{ijkl} e_{kl} - \gamma_{ij} \left(\theta + \tau_1 \dot{\theta}\right), \tag{4.1.3}$$
$$q_i = -K_{ij} \phi_{,j}\,. \tag{4.1.4}$$

**Two-temperature relation:**

$$\left(1 + \tau_1 \frac{\partial}{\partial t}\right) \phi - \left(1 + \tau_1 \frac{\partial}{\partial t}\right) \theta = A_{ij} \phi_{,ij}\,. \tag{4.1.5}$$

**Geometrical relation:**

$$2e_{ij} = 2u_{(i,j)} = (u_{i,j} + u_{j,i}), \tag{4.1.6}$$

where $A_{ij}$ is the temperature discrepancy tensor, $\tau_1$ and $\tau_2$ represent two relaxation times.

Further, the following relaxation times and the material parameters are assumed to carry out:

$$\begin{aligned} &C_{ijkl} = C_{klij} = C_{jikl} = C_{klji}, \quad C_{ijkl}e_{ij}e_{kl} > 0, \quad K_{ij} = K_{ji}, \ \gamma_{ij} = \gamma_{ji}, \\ &C_E > 0, \ \rho > 0, \quad \tau_1 \geq \tau_2 > 0. \end{aligned} \tag{4.1.7}$$

It is also considered that the $K_{ij}, \gamma_{ij}$ and $C_{ijkl}$ are smooth on $\overline{B}$.

The following initial conditions are assumed to the above field equations:

$$\left.\begin{aligned} u_i(x,0) = u_{i0}, \quad \dot{u}_i(x,0) = \dot{u}_{i0}, \quad \theta(x,0) = \alpha_0, \\ \dot{\theta}(x,0) = \alpha_1, \quad e_{ij}(x,0) = e^0_{ij}, \quad \phi(x,0) = \phi_0 \end{aligned}\right\} \tag{4.1.8}$$

and the boundary conditions are taken as

$$\left.\begin{aligned} u_i = \tilde{u}_i \ \text{ on } \ \partial B_1 \times [0,\infty), \\ \sigma_i = \sigma_{ij}n_j = \tilde{\sigma}_i \ \text{ on } \ \partial B_2 \times [0,\infty), \\ \phi = \tilde{\phi} \ \text{ on } \ \partial B_3 \times [0,\infty), \\ q = q_i n_i = \tilde{q} \ \text{ on } \ \partial B_4 \times [0,\infty). \end{aligned}\right\} \tag{4.1.9}$$

Here $u_{i0}$, $\dot{u}_{i0}$, $\alpha_0$, $\alpha_1$, $\phi_0$, $e^0_{ij}$, $\tilde{q}$, $\tilde{\phi}$, $\tilde{u}_i$ and $\tilde{\sigma}_i$ denote the initial values of displacement component, velocity component, thermodynamic temperature, time rate of thermodynamic temperature, conductive temperature, strain component, normal heat flow, conductive temperature, surface displacement component, and traction component, re-

spectively.

The regularity and smoothness conditions are assumed to be as follows:

- $u_{i0}$ is continuously differentiable on $\overline{B}$.
- $\dot{u}_{i0}$, $\alpha_0$, $\alpha_1$, $e^0_{ij}$ and $\phi_0$ are continuous on $\overline{B}$.
- $\tilde{u}_i$ and $\tilde{\phi}$ are continuous on $\partial\overline{B}_1 \times [0,\infty)$ and on $\partial\overline{B_3} \times [0,\infty)$, respectively.
- $\tilde{\sigma}_i$ and $\tilde{q}$ are piecewise continuous on $\partial\overline{B}_2 \times [0,\infty)$ and on $\partial\overline{B}_4 \times [0,\infty)$, respectively.
- $F_i$ and $H$ are continuously differentiable on $\overline{B} \times [0,\infty)$.

Now, functions $u_i$, $e_{ij}$, $\sigma_{ij}$, $\theta$, $\phi$, $q_i$ are introduced by $I = \{u_i,\, e_{ij},\, \sigma_{ij},\, \theta,\, \phi,\, q_i\}$ in an ordered array which is called as an admissible state. The following properties are considered for the constituents of $I$:

- $u_i \in C^{1,2}$, $\theta \in C^{0,2}$, $\phi \in C^{2,1}$, $\sigma_{ij} \in C^{1,0}$, $e_{ij} \in C^{0,1}$, $q_i \in C^{1,0}$.
- $\sigma_{ij} = \sigma_{ji}$, $e_{ij} = e_{ji}$ on $\overline{B} \times [0,\infty)$.

The following operations are defined on admissible state:

1. Addition of admissible states

   $$I + I' = \left\{u_i + u'_i,\, e_{ij} + e'_{ij}, ..., q_i + q'_i\right\}.$$

2. Multiplication of admissible state by a scalar $\chi$

   $$\chi I = \left\{\chi u_i,\, \chi e_{ij}, ..., \chi q_i\right\}.$$

Hence, it is straight forward that the set of all admissible states is a linear space.
If the field Eqs. (4.1.1)-(4.1.6), the initial conditions (4.1.8), and boundary conditions (4.1.9) are satisfied by an admissible state then obviously it is the solution of the mixed initial-boundary value problem.

### 4.1.3 Alternative Formulation

Here we present a formulation of the above mixed problem by incorporating the initial conditions into the field equations in an alternative way. Therefore, we start with the following:

Let $p_1$ and $q_1$ be two continuous functions defined on $\overline{B} \times [0, \infty)$. Then the convolution $p_1 * q_1$ of $p_1$ and $q_1$ is stated by

$$[p_1 * q_1](x,t) = \int_0^t p_1(x, t-\omega)\, q_1(x,\omega)\, d\omega, \quad (x,t) \in \overline{B} \times [0,\infty).$$

The convolution properties are considered, which are as follows:

$$q_1 * p_1 = p_1 * q_1, \tag{4.1.10}$$

$$q_1 * (p_1 + r_1) = (q_1 * p_1) + (q_1 * r_1), \tag{4.1.11}$$

$$q_1 * (p_1 * r_1) = (q_1 * p_1) * r_1 = q_1 * p_1 * r_1, \tag{4.1.12}$$

$$p_1 * q_1 = 0 \implies p_1 = 0 \text{ or } q_1 = 0. \tag{4.1.13}$$

Applying Laplace transform to Eqs. (4.1.1)-(4.1.3), (4.1.5) and using the initial conditions (4.1.8), the following transformed equations are obtained:

$$\bar{\sigma}_{ij,j} + \bar{F}_i = \rho\left(s^2\bar{u}_i - s u_{i0} - \dot{u}_{i0}\right), \tag{4.1.14}$$

$$\rho\bar{H} - \bar{q}_{i,i} = \rho C_E\left[s\bar{\theta} - \alpha_0 + \tau_2\left(s^2\bar{\theta} - \alpha_1 - s\alpha_0\right)\right] + T_0\gamma_{ij}\left(s\bar{e}_{ij} - e^0_{ij}\right), \tag{4.1.15}$$

$$\bar{\sigma}_{ij} = C_{ijkl}\bar{e}_{kl} - \gamma_{ij}\left[\bar{\theta} + \tau_1\left(s\bar{\theta} - \alpha_0\right)\right], \tag{4.1.16}$$

$$A_{ij}\bar{\phi}_{,ij} = \bar{\phi} - \bar{\theta} + \tau_1\left(s\bar{\phi} - \phi_0\right) - \tau_1\left(s\bar{\theta} - \alpha_0\right), \tag{4.1.17}$$

where $s$ is the Laplace transform parameter.

Then applying convolution theorem and the inverse Laplace transform to Eqs. (4.1.14)-

(4.1.17), it is acquired that

$$\rho u_i - g * \sigma_{ij,j} - l_i = 0, \tag{4.1.18}$$

$$\rho C_E \theta + T_0 \gamma_{ij} \dot{G}_0 * e_{ij} + G_0 * q_{i,i} - W = 0, \tag{4.1.19}$$

$$\dot{G}_1 * (\sigma_{ij} - C_{ijkl} e_{kl}) + \gamma_{ij} \theta - m_{ij} = 0, \tag{4.1.20}$$

$$\phi - \theta + M - \dot{G}_1 * A_{ij} \phi_{,ij} = 0, \tag{4.1.21}$$

where, the functions appeared in above equations are denoted on $t \in [0, \infty)$ as follows:

$$G_1(t) = 1 - e^{-t/\tau_1}, \ \dot{G}_1(t) = \frac{1}{\tau_1} e^{-t/\tau_1}, \tag{4.1.22}$$

$$G_0(t) = 1 - e^{-t/\tau_2}, \ \dot{G}_0(t) = \frac{1}{\tau_2} e^{-t/\tau_2}, \tag{4.1.23}$$

$$g(t) = t, \tag{4.1.24}$$

$$m_{ij} = \tau_1 \alpha_0 \gamma_{ij} \dot{G}_1, \tag{4.1.25}$$

$$M = \dot{G}_1 \tau_1 (\alpha_0 - \phi_0). \tag{4.1.26}$$

Moreover, the functions $l_i$ and $W$ on $\overline{B} \times [0, \infty)$ are defined in the following way:

$$l_i = g * F_i + \rho (t \dot{u}_{i0} + u_{i0}), \tag{4.1.27}$$

$$W = G_0 * \rho H + G_0 (\rho C_E \tau_2 \alpha_1 + T_0 \gamma_{ij} \dot{e}_{ij}) + \rho C_E \alpha_0. \tag{4.1.28}$$

Therefore, in view of the above, we obtain the theorem as follows:

**Theorem-4.1.3.1:** The functions $u_i$, $e_{ij}$, $\sigma_{ij}$, $\theta$, $\phi$, $q_i$ satisfy the Eqs. (4.1.1)-(4.1.3), (4.1.5), and the initial conditions (4.1.8) if and only if

$$\rho u_i - g * \sigma_{ij,j} - l_i = 0, \tag{4.1.29}$$

$$\rho C_E \theta + T_0 \gamma_{ij} \dot{G}_0 * e_{ij} + G_0 * q_{i,i} - W = 0, \tag{4.1.30}$$

$$\dot{G}_1 * (\sigma_{ij} - C_{ijkl} e_{kl}) + \gamma_{ij} \theta - m_{ij} = 0, \tag{4.1.31}$$

$$\phi - \theta + M - \dot{G}_1 * A_{ij} \phi_{,ij} = 0. \tag{4.1.32}$$

Furthermore, by making use of this formulation, an alternative description of the mixed problem is obtained, which is as follows:

**Theorem-4.1.3.2:** Let $I = \{u_i,\, e_{ij},\, \sigma_{ij},\, \theta,\, \phi,\, q_i\}$ be an admissible state. Then $I$ is a solution of the mixed problem if and only if it satisfies the Eqs. (4.1.29)-(4.1.32), (4.1.4), (4.1.6), and the boundary conditions (4.1.9).

### 4.1.4 Variational Theorem

Now, a variational theorem under this MTRDTT thermoelasticity theory is formulated in this subsection. A real-valued function is identified as functional where a subset of a linear space is the domain of the function. Now, it is considered that $Z$ be a linear space with subset $Y$ on which a functional $\Omega$ is defined.

Let

$$y, y' \in Y, \quad y + \kappa y' \in Y, \ \ \forall\ \kappa \in \mathbb{R} \tag{4.1.33}$$

and the variation of $\Omega(y)$ at $y$ is defined by

$$\delta_{y'} \Omega\{y\} = \frac{d}{d\kappa} \Omega\{y + \kappa y'\}\Big|_{\kappa=0}. \tag{4.1.34}$$

The variation of $\Omega\{.\}$ is considered to be zero over $Y$ at $y$ in the following way:

$$\delta\Omega\{y\} = 0, \quad \text{over } Y \tag{4.1.35}$$

if and only if $\delta_{y'}\Omega\{y\}$ exists and is equal to zero $\forall\ y'$ consistent with (4.1.33).

**Theorem-4.1.4.1:** Let $J$ be the set of all admissible states. For every $t \in [0,\infty)$ and for each $\Gamma = \{u_i,\, e_{ij},\, \sigma_{ij},\, \theta,\, \phi,\, q_i\} \in J$, the following functional $\Omega_t\{\Gamma\}$ over $J$ is defined:

$$\begin{aligned}
\Omega_t\{\Gamma\} = \int_B \dot{G}_0 * \Big[ g * \Big( \frac{1}{2}\dot{G}_1 * C_{ijkl}e_{kl} + m_{ij} \Big) * e_{ij} + \frac{1}{2}\rho\dot{G}_1 * u_i * u_i \\
- g * \dot{G}_1 * \sigma_{ij} * e_{ij} - \dot{G}_1 * (g * \sigma_{ij,j} + l_i) * u_i \Big]\, dx \\
-\frac{1}{T_0}\int_B g * \Big[ \frac{1}{2}G_0 * \phi_{,j} * K_{ij}\phi_{,j} + \frac{1}{2}\rho C_E\theta * \theta + G_0 * \phi_{,i} * q_i \\
+ (G_0 * q_{k,k} - W) * \theta + T_0\dot{G}_0 * \gamma_{ij}e_{ij} * \theta \Big]\, dx \\
+\frac{G_0}{T_0} * \int_B g * \Big[ M - \dot{G}_1 * A_{ij}\phi_{,ij} \Big] * q_{i,i}dx - \frac{g}{2T_0}A_{ij} * G_0 * \dot{G}_1 * \int_B K_{ij}\phi_{,ij} * \phi_{,ij}\, dx \\
+ \int_{\partial B_1} G_0 * G_1 * \sigma_i * \tilde{u}_i dA \\
+ \int_{\partial B_2} G_0 * G_1 * (\sigma_i - \tilde{\sigma}_i) * u_i dA + \frac{1}{T_0}\int_{\partial B_3} g * G_0 * q * \tilde{\phi} dA \\
+\frac{1}{T_0}\int_{\partial B_4} g * G_0 * (q - \tilde{q}) * \phi dA.
\end{aligned} \tag{4.1.36}$$

Then

$$\delta\Omega_t\{\Gamma\} = 0, \ \ t \in [0,\infty) \tag{4.1.37}$$

if and only if $\Gamma$ satisfies the mixed initial-boundary value problem.

**Proof:** We consider that $\Gamma' = \{u_i',\, e_{ij}',\, \sigma_{ij}',\, \theta',\, \phi',\, q_i'\} \in J$, which concludes that $\Gamma + \kappa\Gamma' \in J$ for every real $\kappa$. Then, from Eqs. (4.1.36), (4.1.10)-(4.1.12), (4.1.34), and the divergence theorem, the following is obtained:

$$
\begin{aligned}
\delta_{\Gamma'}\Omega_t\{\Gamma\} =& \dot{G}_0 * \dot{G}_1 * \int_B (\rho u_i - g * \sigma_{ij,j} - l_i) * u_i' dx \\
&+ g * \dot{G}_0 * \int_B \Big[\dot{G}_1 * (C_{ijkl}e_{kl} - \sigma_{ij}) - \gamma_{ij}\theta + m_{ij}\Big] * e_{ij}' dx \\
&- G_0 * G_1 * \int_B \big[e_{ij} - u_{(i,j)}\big] * \sigma_{ij}' dx \\
&+ \frac{g}{T_0} * \int_B \Big(-G_0 * q_{i,i} + W - T_0\dot{G}_0\gamma_{ij} * e_{ij} - \rho C_E\theta\Big) * \theta' dx \\
&- \frac{g}{T_0} * G_0 * \int_B (K_{ij}\phi_{,j} + q_i) * \phi'_{,j}\, dx \\
&+ \frac{g}{T_0} * G_0 * \int_B \Big(\phi - \theta + M - \dot{G}_1 * A_{ij}\phi_{,ij}\Big) * q_{i,i}' dx \\
&- \frac{gA_{ij}}{T_0} * G_0 * \dot{G}_1 * \int_B (q_{i,i} + K_{ij}\phi_{,ij}) * \phi'_{,ij}\, dx \\
&- G_0 * G_1 * \int_{\partial B_1} (u_i - \tilde{u}_i) * \sigma_i' dA + G_0 * G_1 * \int_{\partial B_2} (\sigma_i - \tilde{\sigma}_i) * u_i' dA \\
&- \frac{g}{T_0} * G_0 * \int_{\partial B_3} \Big(\phi - \tilde{\phi}\Big) * q' dA + \frac{g}{T_0} * G_0 * \int_{\partial B_4} (q - \tilde{q}) * \phi' dA. \qquad (4.1.38)
\end{aligned}
$$

Let us first assume that $\Gamma$ satisfies the present mixed initial-boundary value problem. Then, in view of the Theorem-4.1.3.2, Eq. (4.1.38) along with the suitable $\Gamma'$, Eq. (4.1.37) is satisfied. Thus the first part of this theorem is proved.

Conversely, let Eq. (4.1.37) holds.

Then

$$
\delta_{\Gamma'}\Omega_t\{\Gamma\} = 0,\ t \in [0,\infty),\ \forall\ \Gamma' \in J. \qquad (4.1.39)
$$

The Lemmas $(1)-(3)$ (Gurtin (1964)) are further used.

Since this vanishing occurs for every $\Gamma' \in J$, firstly, it is assumed that $\Gamma' = \{u_i', 0, 0, 0, 0, 0\}$ and let $u_i'$ as well as its all derivatives with respect to space variables vanish on $\partial B \times [0,\infty)$.

Thus, through Eqs. (4.1.38) and (4.1.39), we find that

$$\int_B (\rho u_i - g * \sigma_{ij,j} - l_i) * u_i' dx = 0,\ t \in [0, \infty)\,.$$

Hence, from Eq. (4.1.13) and Lemma 1 (Gurtin (1964)), it is found that Eq. (4.1.29) holds.

Now we consider $\Gamma' = \{u_i', 0, 0, 0, 0, 0\}$ and assume that $u_i'$ vanishes on $\partial B_1 \times [0, \infty)$. Then, from Eqs. (4.1.38)-(4.1.39), (4.1.29) and Lemma 2 (Gurtin (1964)), the following is obtained:

$$(\sigma_i - \tilde{\sigma}_i) = 0 \quad \text{on } \partial B_2 \times [0, \infty)\,.$$

Then Eqs. (4.1.13) and (4.1.22) imply that one of the boundary conditions holds.

In a similar way, by taking convenient choices of $\Gamma'$ and using three lemmas (Lemma 1-3) given in Gurtin (1964), it is obtained that all the other field Eqs. (4.1.30)-(4.1.32), Eqs. (4.1.4) and (4.1.6) and other boundary conditions (4.1.9) hold good. Therefore, it is concluded that $\Gamma$ satisfies Eqs. (4.1.29)-(4.1.32), (4.1.4), (4.1.6) and boundary conditions (4.1.9). Hence, $\Gamma$ satisfies the mixed initial-boundary value problem in view of Theorem-4.1.3.2. Thus, proof of the Theorem-4.1.4.1 is complete as a result of this.

### 4.1.5 Reciprocity Theorem

The reciprocity theorem without the use of Laplace transformation is derived in this subsection. For this, following two different systems of thermoelastic loadings are considered:

$$U^{(n)} = \left(F_i^{(n)}, H^{(n)}, \tilde{u}_i^{(n)}, \tilde{\sigma}_i^{(n)}, \tilde{\phi}^{(n)}, \tilde{q}^{(n)}, u_{i0}^{(n)}, \dot{u}_{i0}^{(n)}, \alpha_0^{(n)}, \alpha_1^{(n)}, e_{ij}^{0(n)}, \phi_0^{(n)}\right),\ n = 1, 2. \tag{4.1.40}$$

Let the two respective thermoelastic configurations be denoted as

$$V^{(n)} = \left(u_i^{(n)}, \phi^{(n)}\right), \quad n = 1, 2. \tag{4.1.41}$$

Then the relation between these two sets of thermoelastic loadings and thermoelastic configurations is derived by the following reciprocity theorem:

**Theorem-4.1.5.1:** Let there be two different systems of thermoelastic loadings $U^{(n)}$, $(n = 1, 2)$ as given by Eq. (4.1.40) and the corresponding thermoelastic configurations are $V^{(n)}$, $(n = 1, 2)$ as given by Eq. (4.1.41). If a thermoelastic solid is subjected to these two thermoelastic loadings then the reciprocal relation holds as follows:

$$\begin{aligned}
&\int_B \left[T_0\dot{G}_0 * \dot{G}_1 * l_i^{(1)} * u_i^{(2)}\right] dx + \int_{\partial B} T_0\dot{G}_0 * \dot{G}_1 * g * \sigma_{ij}^{(1)} * u_i^{(2)} dA \\
&\qquad - \int_B g* \left[T_0\gamma_{ij}\dot{G}_0 * e_{ij}^{(1)} * \theta^{(2)} + T_0\dot{G}_0 * m_{ij}^{(1)} * e_{ij}^{(2)}\right] dx \\
&= \int_B \left[T_0\dot{G}_0 * \dot{G}_1 * l_i^{(2)} * u_i^{(1)}\right] dx + \int_{\partial B} T_0\dot{G}_0 * \dot{G}_1 * g * \sigma_{ij}^{(2)} * u_i^{(1)} dA \\
&\qquad - \int_B g* \left[T_0\gamma_{ij}\dot{G}_0 * e_{ij}^{(2)} * \theta^{(1)} + T_0\dot{G}_0 * m_{ij}^{(2)} * e_{ij}^{(1)}\right] dx,
\end{aligned} \tag{4.1.42}$$

where $l_i^{(n)}$ and $m_{ij}^{(n)}$ $(n = 1, 2)$ are provided by Eqs. (4.1.27) and (4.1.25), respectively.

**Proof:** From Eq. (4.1.20), the following equations for two systems are obtained as:

$$\dot{G}_1 * \sigma_{ij}^{(1)} = \dot{G}_1 * C_{ijkl} e_{kl}^{(1)} - \gamma_{ij}\theta^{(1)} + m_{ij}^{(1)}, \tag{4.1.43}$$

$$\dot{G}_1 * \sigma_{ij}^{(2)} = \dot{G}_1 * C_{ijkl} e_{kl}^{(2)} - \gamma_{ij}\theta^{(2)} + m_{ij}^{(2)}. \tag{4.1.44}$$

By making use of convolution of Eqs. (4.1.43) and (4.1.44) with $e_{ij}^{(2)}$ and $e_{ij}^{(1)}$, respectively and then subtracting, we obtain

$$\dot{G}_1 * \sigma_{ij}^{(1)} * e_{ij}^{(2)} + \gamma_{ij}\theta^{(1)} * e_{ij}^{(2)} - m_{ij}^{(1)} * e_{ij}^{(2)} = \dot{G}_1 * \sigma_{ij}^{(2)} * e_{ij}^{(1)} + \gamma_{ij}\theta^{(2)} * e_{ij}^{(1)} - m_{ij}^{(2)} * e_{ij}^{(1)}. \quad (4.1.45)$$

Again from Eq. (4.1.19), it is obtained that

$$G_0 * q_{i,i}^{(1)} = W^{(1)} - T_0\gamma_{ij}\dot{G}_0 * e_{ij}^{(1)} - \rho C_E\theta^{(1)}, \quad (4.1.46)$$

$$G_0 * q_{i,i}^{(2)} = W^{(2)} - T_0\gamma_{ij}\dot{G}_0 * e_{ij}^{(2)} - \rho C_E\theta^{(2)}. \quad (4.1.47)$$

By making use of convolution of Eqs. (4.1.46) and (4.1.47) with $\theta^{(2)}$ and $\theta^{(1)}$, respectively and then subtracting, we get

$$\begin{aligned} &G_0 * q_{i,i}^{(1)} * \theta^{(2)} + T_0\gamma_{ij}\dot{G}_0 * e_{ij}^{(1)} * \theta^{(2)} - W^{(1)} * \theta^{(2)} \\ &\qquad = G_0 * q_{i,i}^{(2)} * \theta^{(1)} + T_0\gamma_{ij}\dot{G}_0 * e_{ij}^{(2)} * \theta^{(1)} - W^{(2)} * \theta^{(1)}. \end{aligned} \quad (4.1.48)$$

From Eqs. (4.1.45) and (4.1.48), it can be written as

$$\begin{aligned} &T_0\dot{G}_0 * \dot{G}_1 * \sigma_{ij}^{(1)} * e_{ij}^{(2)} + G_0 * q_{i,i}^{(1)} * \theta^{(2)} - T_0\dot{G}_0 * m_{ij}^{(1)} * e_{ij}^{(2)} - W^{(1)} * \theta^{(2)} \\ &= T_0\dot{G}_0 * \dot{G}_1 * \sigma_{ij}^{(2)} * e_{ij}^{(1)} + G_0 * q_{i,i}^{(2)} * \theta^{(1)} - T_0\dot{G}_0 * m_{ij}^{(2)} * e_{ij}^{(1)} - W^{(2)} * \theta^{(1)}. \end{aligned} \quad (4.1.49)$$

Now the following notation is defined:

$$\begin{aligned} L_{mn} = \int_B g * \Big[ &T_0\dot{G}_0 * \dot{G}_1 * \sigma_{ij}^{(m)} * e_{ij}^{(n)} + G_0 * q_{i,i}^{(m)} * \theta^{(n)} \\ &- T_0\dot{G}_0 * m_{ij}^{(m)} * e_{ij}^{(n)} - W^{(m)} * \theta^{(n)} \Big]\, dx, \;\; (m, n = 1, 2)\,. \end{aligned} \quad (4.1.50)$$

Now, using Eqs. (4.1.6), (4.1.8) and (4.1.19), we find after some straight-forward manipulations as

$$\begin{aligned}
&g*\left[T_0\dot{G}_0*\dot{G}_1*\sigma_{ij}^{(m)}*e_{ij}^{(n)}+G_0*q_{i,i}^{(m)}*\theta^{(n)}-T_0\dot{G}_0*m_{ij}^{(m)}*e_{ij}^{(n)}-W^{(m)}*\theta^{(n)}\right]\\
&=T_0\dot{G}_0*\dot{G}_1*g*\left(\sigma_{ij}^{(m)}*u_i^{(n)}\right)_{,j}-T_0\dot{G}_0*\dot{G}_1*\rho u_i^{(m)}*u_i^{(n)}\\
&+T_0\dot{G}_0*\dot{G}_1*l_i^{(m)}*u_i^{(n)}-g*T_0\dot{G}_0*m_{ij}^{(m)}*e_{ij}^{(n)}\\
&-g*T_0\gamma_{ij}\dot{G}_0*e_{ij}^{(m)}*\theta^{(n)}-g*\rho C_E\theta^{(m)}*\theta^{(n)}. \qquad (4.1.51)
\end{aligned}$$

Therefore, from Eqs. (4.1.50) and (4.1.51), we obtain

$$\begin{aligned}
L_{mn}=&\int_B\left[T_0\dot{G}_0*\dot{G}_1*l_i^{(m)}*u_i^{(n)}\right]dx+\int_{\partial B}\left[T_0\dot{G}_0*\dot{G}_1*g*\sigma_{ij}^{(m)}*u_i^{(n)}\right]dA\\
&-\int_B g*\left[\rho C_E\theta^{(m)}*\theta^{(n)}+T_0\gamma_{ij}\dot{G}_0*e_{ij}^{(m)}*\theta^{(n)}+T_0\dot{G}_0*m_{ij}^{(m)}*e_{ij}^{(n)}\right]dx\\
&-\int_B\left[T_0\dot{G}_0*\dot{G}_1*\rho u_i^{(m)}*u_i^{(n)}\right]dx. \qquad (4.1.52)
\end{aligned}$$

Now, Eqs. (4.1.49) and (4.1.50) yield

$$L_{12}=L_{21}. \qquad (4.1.53)$$

Thus, from Eqs. (4.1.52) and (4.1.53), the relation (4.1.42) is acquired. Hence, the proof of Theorem-4.1.5.1 is complete as a result of this.

### 4.1.6 Conclusion

In the present subchapter, some important theorems under MTRDTT thermoelastic model proposed by Shivay and Mukhopadhyay (2019) are established. A characterization of the mixed initial-boundary value problem for homogeneous and anisotropic medium is presented in an alternative way that includes the initial conditions into the

field equations. A convolution type variational principle by using this alternative formulation of the present problem is derived. Also, a reciprocity theorem is established.

## 4.2 Thermoelastic Interactions on Temperature-Rate Dependent Two-Temperature Thermoelasticity in an Infinite Medium Subjected to a Line Heat Source

### 4.2.1 Introduction[2]

In the previous subchapter, some theoretical aspects are discussed under the MTRDTT theorey. In this subchapter, the study of MTRDTT theory is continued by investigating thermoelastic interactions inside an isotropic and homogeneous medium with a continuous line heat source. It is worth recalling that thermoelastic interactions caused by a continuous line heat source were investigated by Sherief and Anwar (1986) in the LS model. Chandrasekharaiah and Murthy (1991) examined thermoelastic interactions resulting from a line heat source in the GL model. Ezzat (1995) also used thermoelasticity theory with two relaxation times to study thermoelastic interactions induced by a line heat source for cylindrical regions. It is also worth mentioning some contributions to the study of thermoelastic interactions resulting from a line heat source (see Dhaliwal et al. (1997), Chandrasekharaiah and Srinath (1998), Prasad et al. (2011)) and one can find that there are significant dissimilarities in the predictions by different models regarding the effects of heat source.

In view of the above, the present subchapter is motivated to discuss thermoelastic interactions under the MTRDTT theory inside an isotropic and homogeneous medium with a continuous line heat source. We study our problem with the unified form of two-temperature relation to compare the results for displacement, temperatures, and stresses under the MTRDTT model with the corresponding results of the

[2]The content of this subchapter is published in ***Zeitschrift für angewandte Mathematik und Physik***, 73, 196 (2022)

two-temperature Green-Lindsay (TTGL) model. The Laplace transform and Hankel transform techniques are applied to solve the problem. Further, through the use of short-time approximation and inverse Laplace transform, the analytical solutions in the space-time domain are obtained. The obtained results are further illustrated numerically and distributions of field variables are depicted in various graphs. Some important observations are highlighted.

### 4.2.2 The Mathematical Model

An isotropic and homogeneous thermoelastic body is considered assuming that there is no body force in the medium. Thus, the governing equations in the context of MTRDTT thermoelasticity theory (Shivay and Mukhopadhyay (2019)) can be written as follows:

**Equation of motion:**

$$\sigma_{ij,j} = \rho \ddot{u}_i. \tag{4.2.1}$$

**Stress-strain temperature relation:**

$$\sigma_{ij} = \lambda e_{kk}\delta_{ij} + 2\mu e_{ij} - \gamma \delta_{ij}\left(1 + \tau_1 \frac{\partial}{\partial t}\right)\theta. \tag{4.2.2}$$

**Strain-displacement relation:**

$$e_{ij} = \frac{1}{2}\left(u_{i,j} + u_{j,i}\right). \tag{4.2.3}$$

**Heat conduction equation including a heat source is considered as:**

$$K\phi_{,ii} = \rho C_E \left(\frac{\partial}{\partial t} + \tau_2 \frac{\partial^2}{\partial t^2}\right)\theta + \gamma T_0 \frac{\partial e}{\partial t} - \rho H. \tag{4.2.4}$$

**Two-temperature relation is expressed as follows:**

$$\left(1+\tau_1 p\frac{\partial}{\partial t}\right)\phi-\left(1+\tau_1 p\frac{\partial}{\partial t}\right)\theta=a\phi_{,ii}, \tag{4.2.5}$$

where $a$ represents the two-temperature parameter and $p$ is a dimensionless parameter that is adopted to express the unified two-temperature relation as

- GL model: $p=a=0$
- TTGL model: $p=0$, $a\neq 0$
- MTRDTT model: $p\neq 0$, $a\neq 0$.

### 4.2.3 Formulation of the Problem

Consider an unbounded thermoelastic solid containing a line heat source. The cylindrical coordinate system $(r,\varphi,z)$ is employed throughout this subchapter. The heat source is assumed to be located along the $z$-axis. We consider that thermoelastic loadings are symmetrical about an axis so that the displacement and temperature vectors will be dependent only on the space variables $r$ and time $t$ having only a radial component. There are two non-zero components of stress tensor, namely $\sigma_{rr}$ and $\sigma_{\varphi\varphi}$, where $\sigma_{rr}$ is in radial direction and $\sigma_{\varphi\varphi}$ denotes the circumferential stress in transverse direction. Further, the strain tensor has the non zero components as

$$e_{rr}=\frac{\partial u}{\partial r},\quad e_{\varphi\varphi}=\frac{u}{r}, \tag{4.2.6}$$

so that the dilatation is given by

$$e=e_{ii}=e_{rr}+e_{\varphi\varphi}=\frac{\partial u}{\partial r}+\frac{u}{r}. \tag{4.2.7}$$

Now, in cylindrical coordinate system, the form of equation of motion (4.2.1) in the present context is given as follows:

$$\frac{\partial \sigma_{rr}}{\partial r} + \frac{\sigma_{rr} - \sigma_{\varphi\varphi}}{r} = \rho \frac{\partial^2 u}{\partial t^2}. \tag{4.2.8}$$

Using Eq. (4.2.7), radial and circumferential stress components will take the forms

$$\sigma_{rr} = \lambda \frac{u}{r} + (\lambda + 2\mu) \frac{\partial u}{\partial r} - \gamma \left(1 + \tau_1 \frac{\partial}{\partial t}\right) \theta, \tag{4.2.9}$$

$$\sigma_{\varphi\varphi} = \lambda \frac{\partial u}{\partial r} + (\lambda + 2\mu) \frac{u}{r} - \gamma \left(1 + \tau_1 \frac{\partial}{\partial t}\right) \theta. \tag{4.2.10}$$

Substituting Eqs. (4.2.9) and (4.2.10) in Eq. (4.2.8), we obtain

$$\rho \frac{\partial^2 u}{\partial t^2} = (\lambda + 2\mu) \left(\frac{\partial^2}{\partial r^2} + \frac{1}{r}\frac{\partial}{\partial r} - \frac{1}{r^2}\right) u - \gamma \left(1 + \tau_1 \frac{\partial}{\partial t}\right) \frac{\partial \theta}{\partial r}. \tag{4.2.11}$$

Further, by combining Eqs. (4.2.4) and (4.2.7), we get

$$K \nabla^2 \phi = \rho C_E \left(\frac{\partial}{\partial t} + \tau_2 \frac{\partial^2}{\partial t^2}\right) \theta + \gamma T_0 \frac{\partial}{\partial t} \left(\frac{\partial u}{\partial r} + \frac{u}{r}\right) - \rho H, \tag{4.2.12}$$

where $\nabla^2 = \frac{\partial^2}{\partial r^2} + \frac{1}{r}\frac{\partial}{\partial r}$.

Now, the following dimensionless transformations will be used for the sake of simplicity:

$$(t', \tau_1', \tau_2') = c_0^2 \eta (t, \tau_1, \tau_2), \quad (r', u') = c_0 \eta (r, u), \quad (\theta', \phi') = \frac{1}{T_0}(\theta, \phi),$$
$$(\sigma_{rr}', \sigma_{\varphi\varphi}') = \frac{1}{(\lambda + 2\mu)} (\sigma_{rr}, \sigma_{\varphi\varphi}), \quad H' = \frac{\gamma H}{K c_0^4 \eta^2},$$

where

$$c_0^2 = \frac{\lambda + 2\mu}{\rho} \text{ and } \eta = \frac{\rho C_E}{K}.$$

In this subchapter, a line heat source is considered which is as follows:

$$H = \frac{1}{2\pi r} R_0 \delta(r) \mathscr{H}(t), \tag{4.2.13}$$

where $R_0$ is a constant, $\mathscr{H}(t)$ is the Heaviside unit step function and $\delta(r)$ represents the Dirac delta function.

Using the Eq. (4.2.13), non-dimensional parameters and variables listed above, Eqs. (4.2.5) and (4.2.9)-(4.2.12) are reduced as follows (by omitting the primes for the sake of simplicity):

$$\frac{\partial^2 u}{\partial t^2} = \left(\frac{\partial^2}{\partial r^2} + \frac{1}{r}\frac{\partial}{\partial r} - \frac{1}{r^2}\right) u - a_1 \left(1 + \tau_1 \frac{\partial}{\partial t}\right) \frac{\partial \theta}{\partial r}, \tag{4.2.14}$$

$$\nabla^2 \phi = \left(\frac{\partial}{\partial t} + \tau_2 \frac{\partial^2}{\partial t^2}\right) \theta + a_2 \frac{\partial}{\partial t} \left(\frac{\partial u}{\partial r} + \frac{u}{r}\right) - \frac{R_0}{2\pi r a_1} \delta(r) \mathscr{H}(t), \tag{4.2.15}$$

$$\sigma_{rr} = \frac{\partial u}{\partial r} + \lambda_1 \frac{u}{r} - a_1 \left(1 + \tau_1 \frac{\partial}{\partial t}\right) \theta, \tag{4.2.16}$$

$$\sigma_{\varphi\varphi} = \frac{u}{r} + \lambda_1 \frac{\partial u}{\partial r} - a_1 \left(1 + \tau_1 \frac{\partial}{\partial t}\right) \theta, \tag{4.2.17}$$

$$\left(1 + \tau_1 p \frac{\partial}{\partial t}\right) \phi - \left(1 + \tau_1 p \frac{\partial}{\partial t}\right) \theta = a_3 \nabla^2 \phi, \tag{4.2.18}$$

where

$$a_1 = \frac{\gamma T_0}{\lambda + 2\mu}, \quad a_2 = \frac{\gamma}{\rho C_E}, \quad a_3 = a c_0^2 \eta^2, \quad \lambda_1 = \frac{\lambda}{\lambda + 2\mu}.$$

### 4.2.4 The Governing Equations in the Laplace Transform Domain

In the present context, the homogeneous initial conditions are considered for all field variables assuming that the body is initially at rest in an unstressed and undeformed state at a constant temperature.

To get the solution, the Laplace transform is used to Eqs. (4.2.14)-(4.2.18). Therefore, we obtain

$$s^2\overline{u} = \left(\frac{\partial^2}{\partial r^2} + \frac{1}{r}\frac{\partial}{\partial r} - \frac{1}{r^2}\right)\overline{u} - a_1\left(1+\tau_1 s\right)\frac{\partial\overline{\theta}}{\partial r}, \tag{4.2.19}$$

$$\nabla^2\overline{\phi} = \left(s+\tau_2 s^2\right)\overline{\theta} + a_2 s\left(\frac{\partial\overline{u}}{\partial r} + \frac{\overline{u}}{r}\right) - \frac{A_1\delta(r)}{rs}, \tag{4.2.20}$$

$$\overline{\sigma}_{rr} = \frac{\partial\overline{u}}{\partial r} + \lambda_1\frac{\overline{u}}{r} - a_1\left(1+\tau_1 s\right)\overline{\theta}, \tag{4.2.21}$$

$$\overline{\sigma}_{\varphi\varphi} = \frac{\overline{u}}{r} + \lambda_1\frac{\partial\overline{u}}{\partial r} - a_1\left(1+\tau_1 s\right)\overline{\theta}, \tag{4.2.22}$$

$$\overline{\theta} = \overline{\phi} - \left(\frac{a_3}{1+\tau_1 ps}\right)\nabla^2\overline{\phi}, \tag{4.2.23}$$

where $A_1 = \frac{R_0}{2\pi a_1}$.

Eliminating $\overline{\theta}$ between Eqs. (4.2.19) and (4.2.23), it is found that

$$\left(\frac{\partial^2}{\partial r^2} + \frac{1}{r}\frac{\partial}{\partial r} - \frac{1}{r^2}\right)\overline{u} - a_1\left(1+\tau_1 s\right)\frac{\partial}{\partial r}\left[\overline{\phi} - \frac{a_3}{1+\tau_1 ps}\left(\frac{\partial^2}{\partial r^2} + \frac{1}{r}\frac{\partial}{\partial r}\right)\overline{\phi}\right] = s^2\overline{u}. \tag{4.2.24}$$

Further, by combining Eqs. (4.2.23) and (4.2.20), the following equation is obtained:

$$\left[1 + \frac{a_3}{1+\tau_1 ps}\left(s+\tau_2 s^2\right)\right]\left(\frac{\partial^2}{\partial r^2} + \frac{1}{r}\frac{\partial}{\partial r}\right)\overline{\phi} = \left(s+\tau_2 s^2\right)\overline{\phi} + a_2 s\left(\frac{\partial\overline{u}}{\partial r} + \frac{\overline{u}}{r}\right) - \frac{A_1\delta(r)}{rs}. \tag{4.2.25}$$

We consider that $D \equiv \frac{\partial}{\partial r}$ and $D^* \equiv \frac{\partial}{\partial r} + \frac{1}{r}$ are two operators.

Therefore, after decoupling of Eqs. (4.2.24) and (4.2.25), we arrive at

$$\left(DD^* - m_1^2\right)\left(DD^* - m_2^2\right)\overline{u} = \left[A_2\left(DD^*\right) - A_3\right]\frac{\partial}{\partial r}\left(\frac{\delta(r)}{r}\right), \tag{4.2.26}$$

$$\left(D^*D - m_1^2\right)\left(D^*D - m_2^2\right)\overline{\phi} = \left[s - \frac{1}{s}\left(D^*D\right)\right]\frac{A_1\delta(r)}{r}. \tag{4.2.27}$$

Here, $A_2 = \frac{a_1 a_3(1+\tau_1 s)A_1}{s(1+\tau_1 ps)}$ and $A_3 = \frac{A_1 a_1(1+\tau_1 s)}{s}$. Furthermore, $m_1^2$ and $m_2^2$ are the roots of

the equation

$$\left(1+b_4 s+b_5 s^2\right) m^4-\left(\varepsilon s+b_1 s^2+b_2 s^3+b_3 s^4\right) m^2+\left(s^3+b_6 s^4+b_7 s^5\right)=0, \quad (4.2.28)$$

where we used the following notations:

$$\begin{aligned}
&b_1=\zeta+1+\tau_1 p\varepsilon, \quad b_2=a_3+\tau_1 p(\zeta+1),\\
&b_3=a_3\tau_2, \quad b_4=\tau_1 p+a_3\varepsilon, \quad b_5=a_3\zeta,\\
&b_6=\tau_1 p+\tau_2, \quad b_7=\tau_1\tau_2 p, \quad \varepsilon=1+a_1 a_2,\\
&\zeta=\tau_2+a_1 a_2\tau_1.
\end{aligned}$$

The solutions to Eqs. (4.2.26) and (4.2.27) that are bounded at infinity can be taken as follows:

$$\overline{u}(r,s)=\frac{1}{m_1^2-m_2^2}\sum_{i=1}^{i=2}(-1)^{i-1} m_i(A_2 m_i^2-A_3)K_1(m_i r), \quad (4.2.29)$$

$$\overline{\phi}(r,s)=\frac{A_1}{m_1^2-m_2^2}\sum_{i=1}^{i=2}(-1)^{i-1}\frac{(m_i^2-s^2)}{s}K_0(m_i r), \quad (4.2.30)$$

where, $K_0(m_i r)$ and $K_1(m_i r)$ denote the modified Bessel function of the second kind having order zero and order one, respectively.

To find the solutions for other field variables, the following identities are used:

$$\nabla^2 K_0(ar)=a^2 K_0(ar), \quad \frac{\partial}{\partial r}K_1(ar)=-aK_0(ar)-\frac{K_1(ar)}{r}. \quad (4.2.31)$$

Therefore, combining Eqs. (4.2.30) and (4.2.23), we get

$$\overline{\theta}(r,s)=\frac{A_1}{m_1^2-m_2^2}\sum_{i=1}^{i=2}(-1)^{i-1}\frac{(m_i^2-s^2)}{s}\left(1-\frac{a_3 m_i^2}{1+\tau_1 ps}\right)K_0(m_i r). \quad (4.2.32)$$

Further, making use of Eqs. (4.2.31) and (4.2.32), Eqs. (4.2.21) and (4.2.22) yield the

following expressions of the stress components in Laplace transform domain:

$$\begin{aligned}\overline{\sigma}_{rr} =&\frac{1}{m_1^2-m_2^2}\sum_{i=1}^{i=2}(-1)^{i-1}\\ &\left\{m_i^2(A_3-A_2m_i^2)+a_1\left(1+\tau_1 s\right)A_1\frac{(s^2-m_i^2)}{s}\left(1-\frac{a_3m_i^2}{1+\tau_1 ps}\right)\right\}K_0(m_ir)\\ &+\frac{1}{m_1^2-m_2^2}\sum_{i=1}^{i=2}(-1)^{i-1}\frac{(1-\lambda_1)}{r}m_i(A_3-A_2m_i^2)K_1(m_ir), \qquad (4.2.33)\\ \overline{\sigma}_{\varphi\varphi} =&\frac{1}{m_1^2-m_2^2}\sum_{i=1}^{i=2}(-1)^{i-1}\\ &\left\{\lambda_1m_i^2(A_3-A_2m_i^2)+a_1\left(1+\tau_1 s\right)A_1\frac{(s^2-m_i^2)}{s}\left(1-\frac{a_3m_i^2}{1+\tau_1 ps}\right)\right\}K_0(m_ir)\\ &+\frac{1}{m_1^2-m_2^2}\sum_{i=1}^{i=2}(-1)^{i-1}\frac{(\lambda_1-1)}{r}m_i(A_3-A_2m_i^2)K_1(m_ir). \qquad (4.2.34)\end{aligned}$$

The system of Eqs. (4.2.29)-(4.2.30) and (4.2.32)-(4.2.34) represents the solutions for displacement, temperatures, and stresses, respectively, in the Laplace transform domain.

### 4.2.5 Short-Time Approximation

For the purpose of obtaining the solutions for the field variables in the space-time domain $(r,t)$, we need to apply the inverse Laplace transform. Since the above equations involve the complicated terms on the Laplace transform parameter $s$, for this reason, it is a challenging task to invert Laplace transform analytically for arbitrary $t$ and to find a closed form analytical solution. Furthermore, the present study is more applicable for the problems concerning short time duration. In view of this, the case of short-time approximation is taken into account and the solution for large $s$ (small value of $t$) is found. Therefore higher power terms of $1/s$ are neglected.

Thus, the approximated roots $m_1$ and $m_2$ of Eq. (4.2.28) in the contexts of the

MTRDTT and TTGL theories are obtained as

$$\left.\begin{aligned} m_1 &\approx a_{10}s + a_{11} + \tfrac{a_{12}}{s}, \\ m_2 &\approx a_{20}(s)^{1/2} + \tfrac{a_{21}}{(s)^{1/2}} + \tfrac{a_{22}}{(s)^{3/2}}, \end{aligned}\right\} \quad \text{for the MTRDTT model} \tag{4.2.35}$$

$$\left.\begin{aligned} m_1 &\approx b_{10}s + b_{11} + \tfrac{b_{12}}{s}, \\ m_2 &\approx b_{20} + \tfrac{b_{21}}{s^2}, \end{aligned}\right\} \quad \text{for the TTGL model} \tag{4.2.36}$$

where

$$\begin{aligned}
a_{10} =& \sqrt{\frac{\tau_2}{\zeta}}, \quad a_{11} = \sqrt{\frac{\tau_2}{\zeta}} \left\{ \frac{\zeta(a_3+\tau_1) - \tau_2(\tau_1 + a_3\varepsilon)}{2\tau_2 a_3 \zeta} \right\}, \\
a_{12} =& \sqrt{\frac{\tau_2}{\zeta}} \left[ \frac{\tau_1^2 \left\{\zeta(-1+4\zeta) - 3\tau_2\right\}(\zeta - \tau_2) - a_3^2(\zeta - \varepsilon\tau_2)(\zeta + 3\varepsilon\tau_2)}{8\zeta^2\tau_2^2 a_3^2} \right. \\
& \left. + \frac{2a_3\left\{2\zeta(\zeta + \zeta\varepsilon\tau_1 - \tau_2)\tau_2 + \tau_1(-\zeta^2 - \zeta(1+\varepsilon+2\zeta\varepsilon)\tau_2 + 3\varepsilon\tau_2^2)\right\}}{8\zeta^2\tau_2^2 a_3^2} \right], \\
a_{20} =& \sqrt{\frac{\tau_1}{a_3}}, \quad a_{21} = \sqrt{\frac{\tau_1}{a_3}} \left( \frac{a_3\tau_2 - \tau_1^2}{2a_3\tau_1\tau_2} \right), \\
a_{22} =& -\sqrt{\frac{\tau_1}{a_3}} \left[ \frac{\tau_1^4(-3+4\zeta-4\tau_2) + a_3^2\tau_2^2 + 2a_3\tau_1^2\left\{(3+2\varepsilon\tau_1)\tau_2 - 2\tau_1(1+\varepsilon\tau_2)\right\}}{8a_3^2\tau_1^2\tau_2^2} \right], \\
b_{10} =& \sqrt{\frac{\tau_2}{\zeta}}, \quad b_{11} = \sqrt{\frac{\tau_2}{\zeta}} \left\{ \frac{\zeta - \tau_2\varepsilon}{2\tau_2\zeta} \right\}, \\
b_{12} =& -\sqrt{\frac{\tau_2}{\zeta}} \left\{ \frac{a_3\varepsilon\tau_2(2\zeta - 3\varepsilon\tau_2) + 4\zeta\tau_2(\tau_2 - \zeta) - a_3\zeta^2}{8\zeta^2\tau_2^2 a_3} \right\}, \\
b_{20} =& \frac{1}{\sqrt{a_3}}, \quad b_{21} = \frac{-1}{\sqrt{a_3}} \left( \frac{1}{2a_3\tau_2} \right).
\end{aligned}$$

Now, substituting the values of $m_1$ and $m_2$ from Eqs. (4.2.35) and (4.2.36) into Eqs. (4.2.29), (4.2.30) and (4.2.32)-(4.2.34) and carrying out the detailed manipulations, we acquire the following short-time approximated expressions for displacement, temperatures, and stresses in the domain of Laplace transform assuming $s$ to be very large:

1. For the MTRDTT model:

$$\overline{u}(r,s) = \left(f_{41} + \frac{f_{42}}{s} + \frac{f_{43}}{s^2}\right) K_1\left((a_{10}s + a_{11})r\right) + \left(\frac{f_{44}}{s^{5/2}}\right) K_1\left(a_{20}s^{1/2}r\right), \tag{4.2.37}$$

$$\overline{\phi}(r,s) = \left(\frac{f_{45}}{s} + \frac{f_{46}}{s^2}\right) K_0\left((a_{10}s + a_{11})r\right) + \left(\frac{f_{47}}{s} + \frac{f_{48}}{s^2}\right) K_0\left(a_{20}s^{1/2}r\right), \tag{4.2.38}$$

$$\overline{\theta}(r,s) = \left(f_{49} + \frac{f_{50}}{s} + \frac{f_{51}}{s^2}\right) K_0\left((a_{10}s + a_{11})r\right) + \left(\frac{f_{52}}{s^2}\right) K_0\left(a_{20}s^{1/2}r\right), \tag{4.2.39}$$

$$\begin{aligned}\overline{\sigma}_{rr}(r,s) = &\left(sf_{53} + \frac{f_{54}}{s} + \frac{f_{55}}{s^2}\right) K_0\left((a_{10}s + a_{11})r\right) \\ &+ \left(\frac{f_{56}}{s} + \frac{f_{57}}{s^2}\right) K_0\left(a_{20}s^{1/2}r\right) \\ &+ \left(f_{58} + \frac{f_{59}}{s} + \frac{f_{60}}{s^2}\right) K_1\left((a_{10}s + a_{11})r\right) + \left(\frac{f_{61}}{s^{5/2}}\right) K_1\left(a_{20}s^{1/2}r\right),\end{aligned} \tag{4.2.40}$$

$$\begin{aligned}\overline{\sigma}_{\varphi\varphi}(r,s) = &\left(sf_{62} + f_{63} + \frac{f_{64}}{s}\right) K_0\left((a_{10}s + a_{11})r\right) \\ &+ \left(\frac{f_{65}}{s} + \frac{f_{66}}{s^2}\right) K_0\left(a_{20}s^{1/2}r\right) \\ &+ \left(f_{67} + \frac{f_{68}}{s} + \frac{f_{69}}{s^2}\right) K_1\left((a_{10}s + a_{11})r\right) + \left(\frac{f_{70}}{s^{5/2}}\right) K_1\left(a_{20}s^{1/2}r\right).\end{aligned} \tag{4.2.41}$$

2. For the TTGL model:

$$\overline{u}(r,s) = \left(sg_{41} + g_{42} + \frac{g_{43}}{s}\right) K_1\left((b_{10}s + b_{11})r\right) + \left(\frac{g_{44}}{s^2} + \frac{g_{45}}{s^3}\right) K_1\left(b_{20}r\right), \tag{4.2.42}$$

$$\overline{\phi}(r,s) = \left(\frac{g_{46}}{s} + \frac{g_{47}}{s^2}\right) K_0\left((b_{10}s + b_{11})r\right) + \left(\frac{g_{48}}{s} + \frac{g_{49}}{s^2}\right) K_0\left(b_{20}r\right), \tag{4.2.43}$$

$$\overline{\theta}(r,s) = \left(sg_{50} + g_{51} + \frac{g_{52}}{s}\right) K_0\left((b_{10}s + b_{11})r\right) + \left(\frac{g_{53}}{s} + \frac{g_{54}}{s^2}\right) K_0\left(b_{20}r\right), \tag{4.2.44}$$

$$\begin{aligned}\overline{\sigma}_{rr}(r,s) = &\left(s^2 g_{55} + s g_{56} + g_{57} + \frac{g_{58}}{s}\right) K_0\left((b_{10}s + b_{11})r\right) \\ &+ \left(g_{59} + \frac{g_{60}}{s} + \frac{g_{61}}{s^2}\right) K_0\left(b_{20}r\right) \\ &+ \left(s g_{62} + g_{63} + \frac{g_{64}}{s}\right) K_1\left((b_{10}s + b_{11})r\right) + \left(\frac{g_{65}}{s^2} + \frac{g_{66}}{s^3}\right) K_1\left(b_{20}r\right),\end{aligned} \tag{4.2.45}$$

$$\begin{aligned}\overline{\sigma}_{\varphi\varphi}(r,s) = &\left(s^2 g_{67} + s g_{68} + g_{69} + \frac{g_{70}}{s}\right) K_0\left((b_{10}s + b_{11})r\right) \\ &+ \left(g_{71} + \frac{g_{72}}{s} + \frac{g_{73}}{s^2}\right) K_0\left(b_{20}r\right) \\ &+ \left(s g_{74} + g_{75} + \frac{g_{76}}{s}\right) K_1\left((b_{10}s + b_{11})r\right) + \left(\frac{g_{77}}{s^2} + \frac{g_{78}}{s^3}\right) K_1\left(b_{20}r\right).\end{aligned} \tag{4.2.46}$$

### 4.2.6 Analytical Results

To find the solutions for short-time approximation in the physical domain $(r,t)$, the following formulae of Laplace inversions (Oberhettinger and Badii (1973)) are used:

$$\begin{aligned}L^{-1}\left[\frac{1}{s^n}\right] &= \frac{t^{n-1}}{(n-1)!}, \\ L^{-1}\left[K_0(asr)\right] &= \frac{\mathscr{H}(t-ar)}{\sqrt{t^2-(ar)^2}}, \;\; L^{-1}\left[\frac{K_0(asr)}{s}\right] = \mathscr{H}(t-ar)\;\; \cosh^{-1}\left(\frac{t}{ar}\right), \\ L^{-1}\left[\frac{K_0(asr)}{s^2}\right] &= \mathscr{H}(t-ar)\left[t\cosh^{-1}\left(\frac{t}{ar}\right) - \sqrt{t^2-(ar)^2}\right], \\ L^{-1}\left[K_1(asr)\right] &= \frac{\mathscr{H}(t-ar)t}{ar\sqrt{t^2-(ar)^2}}, \;\; L^{-1}\left[\frac{K_1(asr)}{s}\right] = \frac{\mathscr{H}(t-ar)}{ar}\sqrt{t^2-(ar)^2}, \\ L^{-1}\left[\frac{K_1(asr)}{s^2}\right] &= \frac{\mathscr{H}(t-ar)}{ar}\left[\frac{t}{2}\sqrt{t^2-(ar)^2} - \frac{(ar)^2}{2}\cosh^{-1}\left(\frac{t}{ar}\right)\right], \\ L^{-1}\left[K_0(ars^{1/2})\right] &= \frac{1}{2t}e^{\frac{-(ar)^2}{4t}}, \;\; L^{-1}\left[\frac{arK_1(ars^{1/2})}{s^{1/2}}\right] = e^{\frac{-(ar)^2}{4t}}.\end{aligned}$$

Finally, applying the inverse Laplace transform to Eqs. (4.2.37)-(4.2.46) and then using the above-mentioned formulae and the convolution theorem of Laplace transform, we arrive at the following solution in physical domain:

1. For the MTRDTT model:

$$\begin{aligned}u(r,t) =&e^{-\alpha_1 t}\left[u_{11}\frac{\mathscr{H}(t-a_{10}r)}{\sqrt{t^2-(a_{10}r)^2}}+u_{12}\mathscr{H}(t-a_{10}r)\sqrt{t^2-(a_{10}r)^2}\right.\\&\left.-u_{13}\mathscr{H}(t-a_{10}r)\ \cosh^{-1}\left(\frac{t}{a_{10}r}\right)\right]+\frac{f_{44}}{a_{20}r}\int_0^t(t-\tau)e^{-\frac{(a_{20}r)^2}{4\tau}}d\tau,\end{aligned}\tag{4.2.47}$$

$$\begin{aligned}\phi(r,t) =&e^{-\alpha_1 t}\left[\phi_{11}\mathscr{H}(t-a_{10}r)\cosh^{-1}\left(\frac{t}{a_{10}r}\right)-\phi_{12}\mathscr{H}(t-a_{10}r)\sqrt{t^2-(a_{10}r)^2}\right]\\&+\frac{f_{47}}{2}\int_0^t\frac{1}{\tau}e^{-\frac{(a_{20}r)^2}{4\tau}}d\tau+\frac{f_{48}}{2}\int_0^t\frac{t-\tau}{\tau}e^{-\frac{(a_{20}r)^2}{4\tau}}d\tau,\end{aligned}\tag{4.2.48}$$

$$\begin{aligned}\theta(r,t) =&e^{-\alpha_1 t}\left[f_{49}\frac{\mathscr{H}(t-a_{10}r)}{\sqrt{t^2-(a_{10}r)^2}}+\theta_{11}\mathscr{H}(t-a_{10}r)\ \cosh^{-1}\left(\frac{t}{a_{10}r}\right)\right]\\&-\theta_{12}\mathscr{H}(t-a_{10}r)\sqrt{t^2-(a_{10}r)^2}\Big]+\frac{f_{52}}{2}\int_0^t\frac{t-\tau}{\tau}e^{-\frac{(a_{20}r)^2}{4\tau}}d\tau,\end{aligned}\tag{4.2.49}$$

$$\begin{aligned}\sigma_{rr}(r,t) =&e^{-\alpha_1 t}\left[f_{53}\int_0^t\delta'(t-\tau)\frac{\mathscr{H}(\tau-a_{10}r)}{\sqrt{\tau^2-(a_{10}r)^2}}d\tau+\sigma_{11}^r\frac{\mathscr{H}(t-a_{10}r)}{\sqrt{t^2-(a_{10}r)^2}}\right.\\&\left.+\sigma_{12}^r\mathscr{H}(t-a_{10}r)\ \cosh^{-1}\left(\frac{t}{a_{10}r}\right)-\sigma_{13}^r\mathscr{H}(t-a_{10}r)\sqrt{t^2-(a_{10}r)^2}\right]\\&+\frac{f_{56}}{2}\int_0^t\frac{1}{\tau}e^{-\frac{(a_{20}r)^2}{4\tau}}d\tau+\frac{f_{57}}{2}\int_0^t\frac{t-\tau}{\tau}e^{-\frac{(a_{20}r)^2}{4\tau}}d\tau+\frac{f_{61}}{a_{20}r^2}\int_0^t(t-\tau)e^{-\frac{(a_{20}r)^2}{4\tau}}d\tau,\end{aligned}\tag{4.2.50}$$

$$\begin{aligned}\sigma_{\varphi\varphi}(r,t) =&e^{-\alpha_1 t}\left[f_{62}\int_0^t\delta'(t-\tau)\frac{\mathscr{H}(\tau-a_{10}r)}{\sqrt{\tau^2-(a_{10}r)^2}}d\tau+\sigma_{11}^{\varphi}\frac{\mathscr{H}(t-a_{10}r)}{\sqrt{t^2-(a_{10}r)^2}}\right.\\&\left.+\sigma_{12}^{\varphi}\mathscr{H}(t-a_{10}r)\ \cosh^{-1}\left(\frac{t}{a_{10}r}\right)-\sigma_{13}^{\varphi}\mathscr{H}(t-a_{10}r)\sqrt{t^2-(a_{10}r)^2}\right]\\&+\frac{f_{65}}{2}\int_0^t\frac{1}{\tau}e^{-\frac{(a_{20}r)^2}{4\tau}}d\tau+\frac{f_{66}}{2}\int_0^t\frac{t-\tau}{\tau}e^{-\frac{(a_{20}r)^2}{4\tau}}d\tau+\frac{f_{70}}{a_{20}r^2}\int_0^t(t-\tau)e^{-\frac{(a_{20}r)^2}{4\tau}}d\tau,\end{aligned}\tag{4.2.51}$$

where $\alpha_1=\frac{a_{11}}{a_{10}}$.

2. For the TTGL model:

$$\begin{aligned}u(r,t) =&e^{-\alpha_2 t}\left[u_{14}\int_0^t \delta'(t-\tau)\frac{\tau\mathscr{H}(\tau-b_{10}r)}{\sqrt{\tau^2-(b_{10}r)^2}}d\tau + u_{15}\frac{\mathscr{H}(t-b_{10}r)}{\sqrt{t^2-(b_{10}r)^2}}\right.\\ &\left.+ u_{16}\mathscr{H}(t-b_{10}r)\sqrt{t^2-(b_{10}r)^2}\right] + u_{17}e^{-b_{20}r}, \qquad (4.2.52)\\ \phi(r,t) =&e^{-\alpha_2 t}\left[\phi_{13}\mathscr{H}(t-b_{10}r)\,\cosh^{-1}\left(\frac{t}{b_{10}r}\right) - \phi_{14}\mathscr{H}(t-b_{10}r)\sqrt{t^2-(b_{10}r)^2}\right]\\ &+\phi_{15}e^{-b_{20}r}, \qquad (4.2.53)\\ \theta(r,t) =&e^{-\alpha_2 t}\left[g_{50}\int_0^t \delta'(t-\tau)\frac{\mathscr{H}(\tau-b_{10}r)}{\sqrt{\tau^2-(b_{10}r)^2}}d\tau + \theta_{13}\frac{\mathscr{H}(t-b_{10}r)}{\sqrt{t^2-(b_{10}r)^2}}\right]\\ &+\theta_{14}\mathscr{H}(t-b_{10}r)\;\cosh^{-1}\left(\frac{t}{b_{10}r}\right)\Bigg] + \theta_{15}e^{-b_{20}r}, \qquad (4.2.54)\end{aligned}$$

$$\begin{aligned}\sigma_{rr}(r,t) =&e^{-\alpha_2 t}\left[g_{55}\int_0^t \delta''(t-\tau)\frac{\mathscr{H}(\tau-b_{10}r)}{\sqrt{\tau^2-(b_{10}r)^2}}d\tau + \sigma_{14}^r\int_0^t \delta'(t-\tau)\frac{\mathscr{H}(\tau-b_{10}r)}{\sqrt{\tau^2-(b_{10}r)^2}}d\tau\right.\\ &+\sigma_{15}^r\int_0^t \delta'(t-\tau)\frac{\tau\mathscr{H}(\tau-b_{10}r)}{\sqrt{\tau^2-(b_{10}r)^2}}d\tau + \sigma_{16}^r\frac{\mathscr{H}(t-b_{10}r)}{\sqrt{t^2-(b_{10}r)^2}}\\ &\left.+ g_{58}\mathscr{H}(t-b_{10}r)\;\cosh^{-1}\left(\frac{t}{b_{10}r}\right) - \frac{g_{64}}{b_{10}r^2}\mathscr{H}(t-b_{10}r)\sqrt{t^2-(b_{10}r)^2}\right] + \sigma_{17}^r e^{-b_{20}r},\end{aligned} \qquad (4.2.55)$$

$$\begin{aligned}\sigma_{\varphi\varphi}(r,t) =&e^{-\alpha_2 t}\left[g_{67}\int_0^t \delta''(t-\tau)\frac{\mathscr{H}(\tau-b_{10}r)}{\sqrt{\tau^2-(b_{10}r)^2}}d\tau + \sigma_{14}^\varphi\int_0^t \delta'(t-\tau)\frac{\mathscr{H}(\tau-b_{10}r)}{\sqrt{\tau^2-(b_{10}r)^2}}d\tau\right.\\ &+\sigma_{15}^\varphi\int_0^t \delta'(t-\tau)\frac{\tau\mathscr{H}(\tau-b_{10}r)}{\sqrt{\tau^2-(b_{10}r)^2}}d\tau + \sigma_{16}^\varphi\frac{\mathscr{H}(t-b_{10}r)}{\sqrt{t^2-(b_{10}r)^2}}\\ &\left.+ g_{70}\mathscr{H}(t-b_{10}r)\;\cosh^{-1}\left(\frac{t}{b_{10}r}\right) - \frac{g_{76}}{b_{10}r^2}\mathscr{H}(t-b_{10}r)\sqrt{t^2-(b_{10}r)^2}\right] + \sigma_{17}^\varphi e^{-b_{20}r},\end{aligned} \qquad (4.2.56)$$

where $\alpha_2 = \frac{b_{11}}{b_{10}}$.

These expressions (4.2.47)-(4.2.56) denote the final short-time approximated solutions

in the domain $(r, t)$.

### 4.2.7 Analysis of the Analytical Results

In this subsection, the solutions for short-time approximation discussed above are examined. From the solution as given by (4.2.47)-(4.2.56), one can clearly observe that the solution of each field variable is made up of two distinct parts. The first part, which includes the term $\mathscr{H}(t - a_{10}r)$, expresses the role of an elastic wave that propagates with finite speed $1/a_{10}$ near the wavefront $r = \frac{t}{a_{10}}$. Also, this wave decays exponentially and the decaying exponent is found to be strongly influenced by the dimensionless two-temperature parameter $a_3$. It is also concluded that the velocity of elastic waves depends on the thermal relaxation parameters as well as other thermoelastic parameters. The rest part of the solution does not contribute to any wave but this part was also found to be dependent on the dimensionless two-temperature parameter $a_3$.

Like the case of MTRDTT model, the first part of solutions in the TTGL model also contains the term $\mathscr{H}(t - b_{10}r)$ which expresses the role of an elastic wave nearby the wavefront $r = \frac{t}{b_{10}}$ and propagates with finite speed $1/b_{10}$. As opposed to the MTRDTT model, the decaying exponent in the first term does not depend on the dimensionless two-temperature parameter $a_3$. Similar to the MTRDTT model, another part of the solution makes no contribution to any wave, but it is dependent on the dimensionless two-temperature parameter $a_3$. Therefore, the propagation speed is not finite for thermal waves in the two-temperature models.

Moreover, we conclude that the conductive temperature is continuous under the MTRDTT model and TTGL model, whereas other field variables including displacement, thermodynamic temperature, and stresses are discontinuous in nature with an infinite discontinuity at the elastic wave front.

Further comparison of the above results with the corresponding results as obtained by Chandrasekharaiah and Murthy (1991) and also by Ezzat (1995) for the case of GL

model, a significant difference is observed with the results predicted by MTRDTT and TTGL models. The solution of each field variable in the GL model, unlike the MTRDTT and TTGL models, consists of two waves decaying exponentially and each wave propagates with finite speed. Moreover, at both the elastic and thermal wave fronts, the temperature distribution shows discontinuity with finite jumps and the stresses $\sigma_{rr}$ and $\sigma_{\varphi\varphi}$ show infinite discontinuity in the case of GL model (Chandrasekharaiah and Murthy (1991), Ezzat (1995)). Such significant dissimilarity in the prediction of two-temperature model as compared to the GL model is an important investigation of the present subchapter.

### 4.2.8 Numerical Results and Discussion

To gain a more in-depth understanding of the behavior of short-time approximated solutions including heat sources, as well as to graphically represent the analytical findings, we carry out numerical work using computational tool MATLAB. Throughout this computations, the copper material is considered. The values of physical parameters and material constants are taken as (Shivay and Mukhopadhyay (2019))

$$\lambda = 7.76 \times 10^{10} \text{ N m}^{-2},\ \mu = 3.86 \times 10^{10} \text{ N m}^{-2},\ C_E = 383.1 \text{ J kg}^{-1} \text{ K}^{-1},$$
$$T_0 = 293 \text{ K},\ \rho = 8954 \text{ kg m}^{-3},\ R_0 = 1 \text{ W m}^{-2},\ \alpha_t = 1.78 \times 10^{-5} \text{ K}^{-1},$$
$$K = 386 \text{ W m}^{-1} \text{ K}^{-1},\ \tau_1 = 0.15,\ \tau_2 = 0.10.$$

The variations of these field quantities with respect to radial distance $r$ are presented in different figures. The computation of these field variables is carried out under two different thermoelastic models, namely, the MTRDTT model and the TTGL model. The parts (a) and (b) of each figure are used to exhibit the figures independently. The part (a) in all the figures shows the effect of a non-dimensional two-temperature parameter ($a_3$) on the field quantities at a particular time $t = 0.4$, whereas part (b)

displays the variation of field variables at various instants of time ($t = 0.25, 0.45, 0.65$) for $a_3 = 0.6$. Our numerical results reveal that at the origin, all field variables have an infinite jump, where the heat source is located. According to our observations, the dimensionless speed of elastic waves is 1.0125 for both models. It is further observed that all the field variables decrease to zero beyond the elastic wave front at any time. This completely agrees with the corresponding theoretical results provided in Eqs. (4.2.47)-(4.2.56). We also come across the following observations:

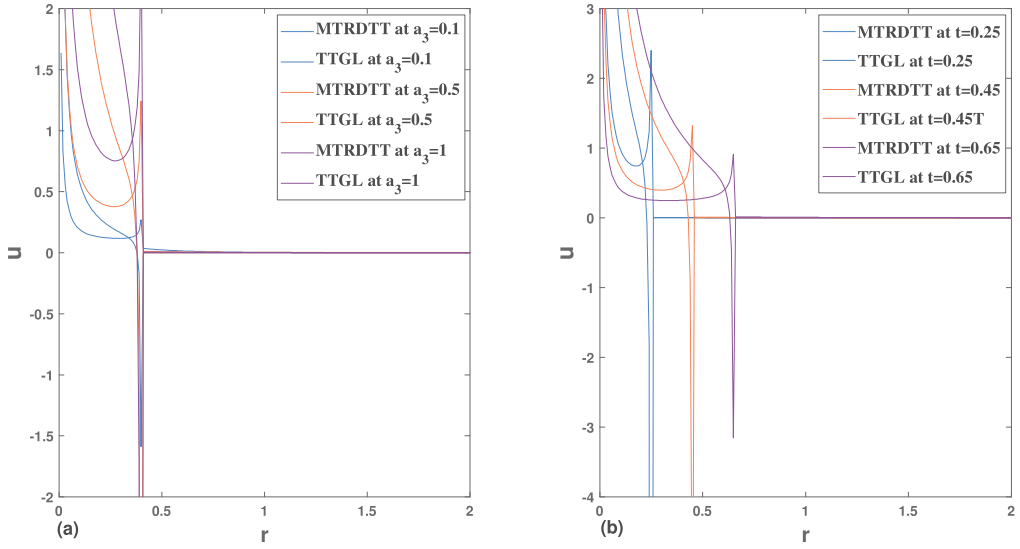


Figure 4.2.1: (a) Variation of $u$ along $r$ at $t = 0.4$. (b) Variation of $u$ along $r$ at $a_3 = 0.6$.

Fig. 4.2.1(a) shows the nature of displacement for the three different values of $a_3$ ($a_3 = 0.1, 0.5, 1$) with respect to radial distance $r$, whereas Fig. 4.2.1(b) displays the variation of displacement at different values of time ($t = 0.25, 0.45, 0.65$) with respect to $r$. From Figs. 4.2.1(a,b), it is concluded that as $r$ increases, displacement decreases from a very high value to zero for both models. However, just behind the elastic wavefront location, the displacement begins to rise abruptly and reaches a high positive value and jumps down to zero in the case of MTRDTT model. On the other hand, the displacement suddenly decreases to a high negative value just near the elastic wavefront location and then jumps up to zero value in the case of TTGL model. This is due to the

impact of impulsive heat source. We further observe that as the value of $a_3$ increases, the displacement increases and decreases in the cases of MTRDTT model and TTGL model, respectively. Hence, the two-temperature parameter has a prominent effect. This is clearly verified in Fig. 4.2.1(a). Fig. 4.2.1(b) verifies that behind the position of wave front, the displacement component attains a higher value at the initial time of interaction (i.e., for smaller values of time). However, no disturbance has been observed for both models after the elastic wavefront location. Thus, a significant difference is observed in the results predicted by the MTRDTT and TTGL models for displacement near the location of the elastic wave front.

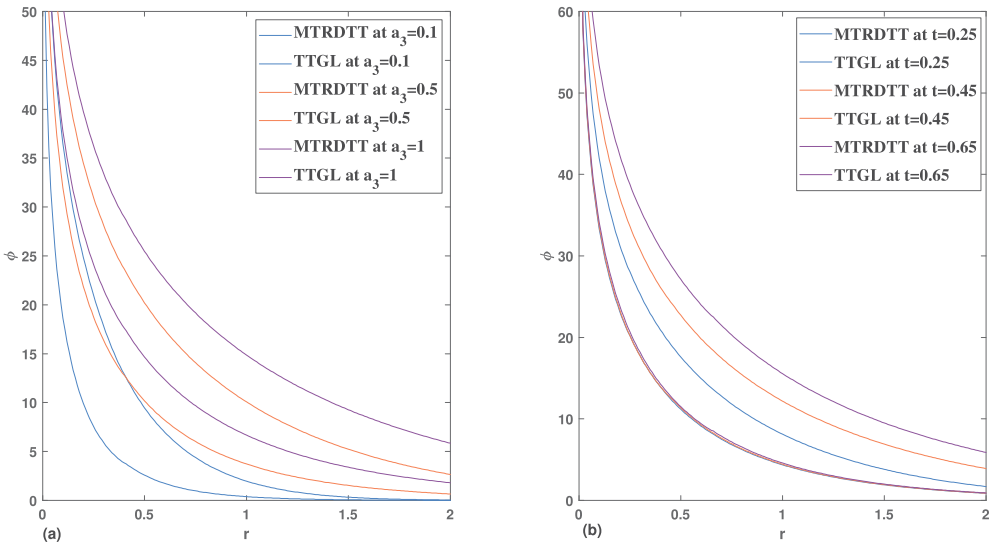


Figure 4.2.2: (a) Variation of $\phi$ along $r$ at $t = 0.4$. (b) Variation of $\phi$ along $r$ at $a_3 = 0.6$.

The distribution of conductive temperature ($\phi$) along the radial distance is depicted in Figs. 4.2.2(a,b). Fig. 4.2.2(a) and Fig. 4.2.2(b) describe the variations of conductive temperature along with $r$ for various values of $a_3$ ($a_3 = 0.1, 0.5, 1$) and time ($t = 0.25, 0.45, 0.65$), respectively in the contexts of MTRDTT and TTGL models. Figs. 4.2.2(a,b) show the similar nature of conductive temperature for the MTRDTT and TTGL models demonstrating that $\phi$ for both the models begins with infinite value and then, decreases to zero as $r$ increases. Therefore, this field has a decreasing nature.

It can be seen that the value of temperature is higher for the MTRDTT model in comparison to the TTGL model. From Fig. 4.2.2(a), it is further observed that conductive temperature increases as the value of $a_3$ increases for both the models. This indicates that parameter $a_3$ has a prominent effect on both models. Moreover, Fig. 4.2.2(b) reports that the value of $\phi$ also increases with the increasing value of $t$ in the case of MTRDTT model. In contrast, the value of $\phi$ remains the same for different values of time in the case of TTGL model. Furthermore, conductive temperature follows almost a similar trend under the MTRDTT and TTGL models at a given time.

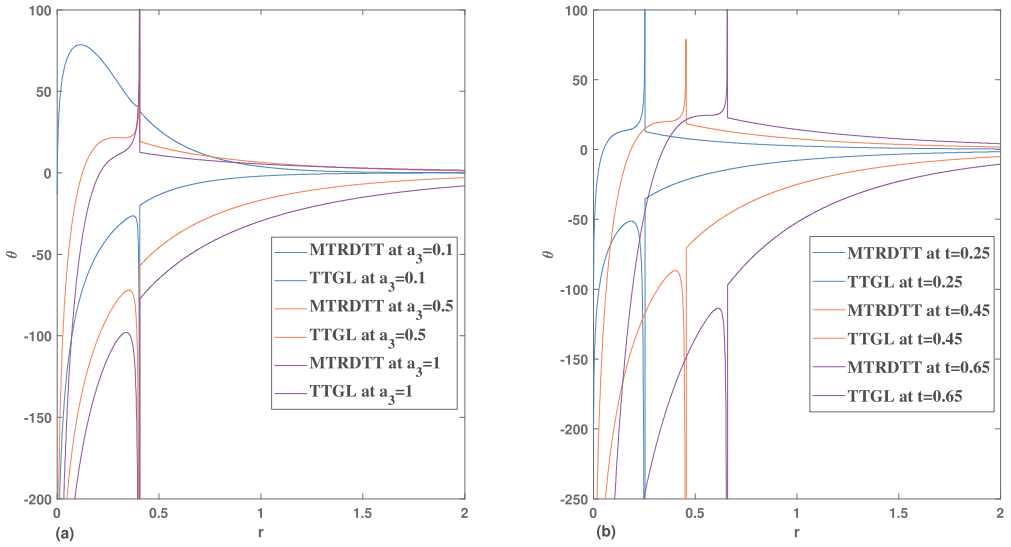


Figure 4.2.3: (a) Variation of $\theta$ along $r$ at $t = 0.4$. (b) Variation of $\theta$ along $r$ at $a_3 = 0.6$.

Figs. 4.2.3(a,b) represent the variation of thermodynamic temperature ($\theta$) with respect to $r$ for MTRDTT and TTGL models. From Figs. 4.2.3(a,b), it is observed that under the MTRDTT model, the thermodynamic temperature increases from a negative infinity value, reaches a high value at the position of elastic wave front and then jumps down to zero. At the same time, starting from a negative infinity value, $\theta$ increases as $r$ increases and just before the elastic wave front, abruptly decreases to a high negative value and then approaches zero in view of the TTGL model. This field shows an infinite discontinuity at the wave front under both models. This is clearly

verified from Fig. 4.2.3(a) that before the position of elastic wavefront, $\theta$ decreases as the value of $a_3$ increases and it tends to zero after the elastic wavefront under both the models. Fig. 4.2.3(b) discusses the variation of thermodynamic temperature at different instants of time and indicates that $\theta$ near the elastic wave front behaves differently with time. In the context of MTRDTT model, $\theta$ increases before the elastic wave front as time increases, whereas $\theta$ has a decreasing trend for the case of TTGL model. Hence, we conclude that for this field variable, the MTRDTT model predicts prominently different behavior in comparison to the TTGL model.

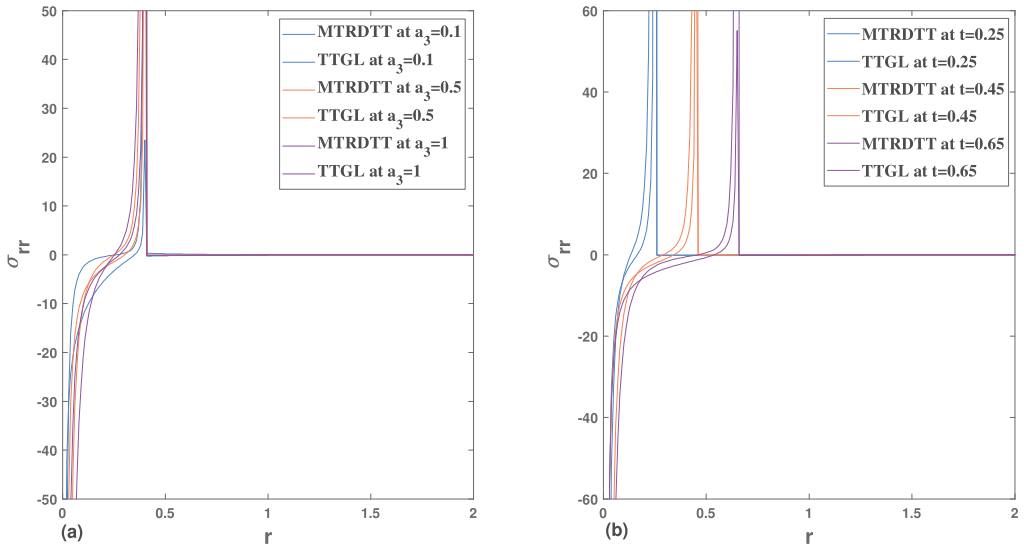


Figure 4.2.4: (a) Variation of $\sigma_{rr}$ along $r$ at $t = 0.4$. (b) Variation of $\sigma_{rr}$ along $r$ at $a_3 = 0.6$.

The variation of radial stress ($\sigma_{rr}$) in the contexts of MTRDTT and TTGL models is illustrated by Figs. 4.2.4(a,b). Fig. 4.2.4(a) depicts the variation of radial stress for various values of $a_3$, whereas the variation of radial stress for different values of $t$ is presented in Fig. 4(b). Figs. 4(a,b) indicate that the radial stress under the MTRDTT and TTGL models behave similarly. From Figs. 4.2.4(a,b), it is seen that under the MTRDTT model, the radial stress increases from a negative infinity value, attains a very high positive value and then decreases to a zero value. This variation trend in $\sigma_{rr}$

is very similar to the TTGL model. Therefore, it is concluded that $\sigma_{rr}$ is an increasing function of $r$ under both the models before the location of wave front. We further notice that $\sigma_{rr}$ increases with the increase of $a_3$ at the wave front location which is also clear in Fig. 4.2.4(a). From Fig. 4.2.4(b), it is observed that $\sigma_{rr}$ attains a higher value at the wave front position at the initial time. Under both these theories, the radial stress field shows an infinite discontinuity at the wave front. Finally, we observe that the trend of radial stress under the MTRDTT model agrees with the TTGL model.

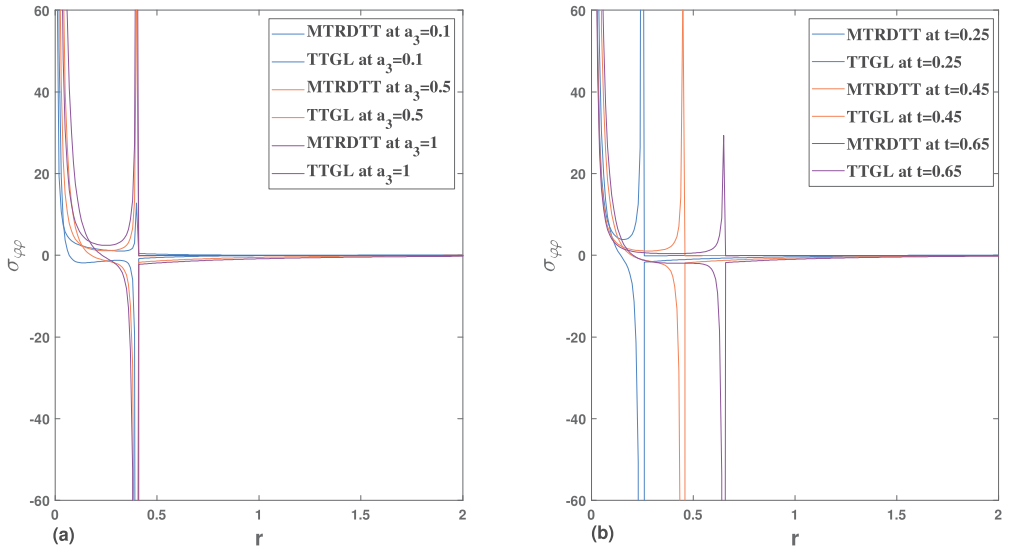


Figure 4.2.5: (a) Variation of $\sigma_{\varphi\varphi}$ along $r$ at $t = 0.4$. (b) Variation of $\sigma_{\varphi\varphi}$ along $r$ at $a_3 = 0.6$.

Figs. 4.2.5(a,b) demonstrate the variations of circumferential stress ($\sigma_{\varphi\varphi}$) along with to $r$ for various values of $a_3$ and time, respectively. From Figs. 4.2.5(a,b), it can be seen that the circumferential stress for the MTRDTT model begins to decrease from a positive infinity value and just before the elastic wave front, it suddenly increases to a high positive value and then jumps to zero. However, the behavior of $\sigma_{\varphi\varphi}$ under the MTRDTT model is quite different as compared to the TTGL model indicating that $\sigma_{\varphi\varphi}$ decreases with increasing $r$ and jumps up to zero value after attaining a high negative value at the elastic wave front. This fact is also clearly verified in Figs. 4.2.5(a,b). Also,

from Fig. 4.2.5(a), it is found that the $\sigma_{\varphi\varphi}$ increases as $a_3$ increases under the MTRDTT model, however, $\sigma_{\varphi\varphi}$ decreases with the increasing value of $a_3$ under the TTGL model. Furthermore, as shown in Fig. 4.2.5(b), the trend of variation of $\sigma_{\varphi\varphi}$ changes with time near the elastic wave front for both the models. We finally conclude that the profile of circumferential stress for the MTRDTT model differs from the case of the TTGL model implying that the effects of temperature rate terms in two-temperature relation play a significant role in the thermoelastic interactions due to the presence of a heat source inside the medium.

### 4.2.9 Conclusion

In this subchapter, the thermoelastic interactions inside an isotropic and homogeneous medium using the MTRDTT and TTGL thermoelastic models in the presence of a continuous line heat source are investigated. In order to investigate the effect of heat source on the field variables, the short-time approximated solutions are derived. To compare the outcomes predicted by the MTRDTT model and the TTGL model, the unified two-temperature relation is employed to study our problem. The theoretical results under both the models (MTRDTT and TTGL) are graphically displayed for a suitable example. Several important facts about the behavior of these field variables are highlighted. Some of these details can be categorized as follows:

- Unlike the GL model that predicts finite speed for elastic as well as for thermal waves, the short-time approximated solutions obtained in the MTRDTT model and TTGL model clearly show that the solution for each field is divided into two distinct parts. The first part expresses the role of an elastic wave propagating with finite speed, whereas the rest part of the solution does not contribute to any wave under both the models. This signifies the fact that the temperature-rate dependent two-temperature models do not admit finite wave speed of the thermal wave.

- In the same way as in the GL model, the effect of heat source under the MTRDTT and TTGL models are limited to a bounded but time-dependent region of space around it.

- Except for the conductive temperature, which is continuous in both models, rest of the field variables show discontinuity at the elastic wave-front.

- For displacement, temperature, and circumferential stress fields, the difference between MTRDTT and TTGL models seems to be more apparent. However, in the case of radial stress, it is investigated that the variation of $\sigma_{rr}$ is similar in nature under both the models.

- As the value of $a_3$ increases, the value of all the field variables at the position of wave front increases under the MTRDTT model. As opposed to the MTRDTT model, the value of $u$, $\theta$, and $\sigma_{\varphi\varphi}$ decrease with the increasing value of $a_3$ at the position of wave front in the context of TTGL model. However, as with the MTRDTT model, the value of $\phi$ and $\sigma_{rr}$ increase with the increasing value of $a_3$ in the TTGL model.

- The two-temperature parameter on all the field variables has a prominent effect on both the models. It is worth to be mentioned here that the effect of this modified two-temperature relation indicates a clear difference in the corresponding results predicated by the present models.